First publ. in: Biochemistry 37 (1998), 7, pp. 1848-1860

Substrate Activation by Acyl-CoA Dehydrogenases: Transition-State Stabilization and p*K*s of Involved Functional Groups[†]

Petra Vock, Stefan Engst, Michael Eder, and Sandro Ghisla*

Faculty of Biology, University of Konstanz, P.O. Box 5560-M644, D-78457 Konstanz, Germany

ABSTRACT: The mechanism by which acyl-CoA dehydrogenases initiate catalysis was studied by using *p*-substituted phenylacetyl-CoAs (substituents -NO_2, -CN, and CH_3CO-), 3S-C_8-, and 3′-dephospho-3S-C_8CoA. These analogues lack a βC−H and cannot undergo α,β-dehydrogenation. Instead they deprotonate at αC−H at pH ≥ 14 to form delocalized carbanions having strong absorbancies in the near UV−visible spectrum. The pK_as of the corresponding phenylacetone analogues were determined as ≈13.6 (-NO_2), ≈14.5 (-CN), and ≈14.6 (CH_3CO-). Upon binding to human wild-type medium-chain acyl-CoA dehydrogenase (MCADH), all analogues undergo αC−H deprotonation. While the extent of deprotonation varies, the anionic products form charge-transfer complexes with the oxidized flavin. From the pH dependence of the dissociation constants (K_d) of *p*-NO_2-phenylacetyl-CoA (4NPA-CoA), 3S-C_8-CoA, and 3′-dephospho-3S-C_8CoA, four pK_as at ≈5, ≈6, ≈7.3, and ≈8 were identified. They were assigned to the following ionizations: (a) pK_a ≈5, ligand (L−H) in the MCADH∼ligand complex; (b) pK_a ≈6, Glu376-COOH in uncomplexed MCADH; (c) pK_a ≈7.3, Glu99-COOH in uncomplexed MCADH (Glu99 is a residue that flanks the bottom of the active-center cavity; this p*K* is absent in the mutant Glu99Gly-MCADH); and (d) p*K* ≈8, Glu99-COOH in the MCADH∼4NPA-CoA complex. The pK_a ≈6 (b) is not significantly affected in the MCADH∼4NPA-CoA complex, but it is increased by ≥1 p*K* unit in that with 3S-C_8CoA and further in the presence of C_8-CoA, the best substrate. The αC−H pK_as of 4NPA-CoA, of 3S-C_8-CoA, and of 3′-dephospho-3S-C_8CoA in the complex with MCADH are ≈5, ≈5, and ≈6. Compared to those of the free species these pK_a values are therefore lowered by 8 to ≥11 pH units (50 to ≥ 65 kJ mol^{-1}) and are close to the pK_a of Glu376-COOH in the complex with substrate/ligand. This effect is ascribed mainly to the hydrogen-bond interactions of the thioester carbonyl group with the ribityl-2′-OH of FAD and Glu376-NH. It is concluded that the pK_a shifts induced with normal substrates such as *n*-octanoyl-CoA are still higher and of the order of 9−13 p*K* units. With 4NPA-CoA and MCADH, αC−H abstraction is fast (k_{app} ≈55 s^{-1} at pH 7.5 and 25 °C, deuterium isotope effect ≈1.34). However, it does not proceed to completion since it constitutes an approach to equilibrium with a finite rate for reprotonation in the pH range 6−9.5. The extent of deprotonation and the respective rates are pH-dependent and reflect apparent pK_as of ≈5 and ≈7.3, which correspond to those determined in static experiments.

Acyl-CoA dehydrogenases catalyze the α,β-dehydrogenation of fatty acid acyl-CoA conjugates to their corresponding enoyl-CoA products; the redox equivalents formed in this reaction are transferred to electron transferring flavoprotein and further to the respiratory chain (*1*, *2*). A peculiarity of the α,β-dehydrogenation reaction is that it involves the concomitant fission of two kinetically stable C−H bonds. In the past, studies with medium-chain acyl-CoA dehydrogenase (MCADH)[1] have led to considerable insight concerning the mechanism of this reaction. It proceeds via an anti elimination where the *pro*(*R*)-α-proton is abstracted by the active-site base Glu376, and the β-hydrogen (*3*, *4*) is transferred as hydride to the flavin N(5) position (*5*). This process is most probably concerted, as inferred from the multiplication of deuterium isotope effects observed using substrates selectively deuterated at the α- and β-positions and at both of them (*6*). The MCADH-catalyzed rate of dehydrogenation (and thus α-deprotonation) of the best substrate, *n*-octanoyl-CoA, is ≈320 s^{-1} at 5 °C (*7*) and >1000 s^{-1} at 25 °C (unpublished results). The α-proton is only weakly acidic in an aqueous environment and a pK_a value of ≈21 has been estimated (*8*, *9*). Glu376, the general base, on the other hand, is only weakly basic and has a pK_a close to neutral. To explain the high catalytic rate, considerable substrate activation, which effectively decreases the pK_a of the α-proton and is equivalent to the stabilization of an

[†] Supported by grants from the Deutsche Forschungsgemeinschaft (Gh 2/4-7, Gh 2/6-1) to S.G. Presented in part at the 10th Symposium on Flavins and Flavoproteins; Como (1991) (*23*).

* Address correspondence to this author: Tel +497531 882291; Fax +497531 884161; E-Mail Sandro.Ghisla@uni-konstanz.de.

[1] Abbreviations: hwtMCADH, recombinant human wild-type medium-chain acyl-CoA dehydrogenase (E.C. 1.3.99.3); Glu99Gly- or E99G-MCADH, Glu99Gly mutant of medium-chain acyl-CoA dehydrogenase; LCADH, recombinant human wild-type long-chain acyl-CoA dehydrogenase (E.C. 1.3.99.13); 4NPA-CoA, (4-nitrophenyl)acetyl-coenzyme A; 4CNPA-CoA, (4-cyanophenyl)acetyl-coenzyme A; 4AcPA-CoA, (4-acetylphenyl)acetyl-coenzyme A; 3S-C_8CoA, 3-thiaoctanoyl-coenzyme A; L−H, acyl-CoA ligand having an ionizable αC−H function; K_L, dissociation constant of ligand; K_{E-H} and $K_{E\sim L-H}$, ionization constants of enzyme functional group and bound ligand.

enolate-like intermediate species, has to occur. In the past, similar arguments have been made for analogous enzyme systems that are involved in the deprotonation of α-carbon acid substrates (*10*).

In the case of the acyl-CoA dehydrogenases, more than 3 decades ago Cornforth (*11*) postulated that a specific interaction with the thioester functional group might increase the acidity of the αC−H position. This mode of activation has been verified in a series of different approaches. Engel and Massey (*12*) first demonstrated that acetoacetyl-CoA binds in its anionic form to bacterial butyryl-CoA dehydrogenase. Various substrates and analogues undergo exchange of the αC−H with solvent-borne hydrogen isotopes in the presence of MCADH (*5, 13*). The same enzyme catalyzes the rearrangement of double bonds in unsaturated acyl-CoAs (*12, 14*). Furthermore a number of substrate analogues that are blocked in *β*-position and thus cannot undergo hydride transfer are stabilized in their α-deprotonated form upon binding to pig kidney MCADH. Compounds that fall under this category are *trans*-3-enoyl-CoA (*15*), 3-oxaoctanoyl-CoA, and 3S-C_8CoA (*16*). The three-dimensional structure of pig kidney MCADH indicates that the substrate thioester carbonyl oxygen participates in two hydrogen bonds, one with the 2′-OH group of the ribityl side chain of the FAD cofactor and one with the N−H backbone of Glu376 (distances 2.8 and 3.0 Å) (*17*). When normal FAD is replaced with 2′-deoxy-FAD in pig kidney MCADH, no catalytic activity is detectable in the standard assay; in single-turnover experiments, the rate of reduction of the flavin cofactor, which is assumed to reflect substrate αC−H deprotonation, is decreased ≈10^7-fold (*18, 19*). The stretching vibrations of the carbonyl moiety of bound 2-enoyl-CoA measured in Raman experiments (*20*) and the effects in the spectra of substrate analogues (*21*) are fully compatible with the proposed type of strong interaction. Thus, while the basic mode of interaction seems to be unquestioned, the extent to which the substrate (and analogue) αC−H is acidified upon binding to the active site has not yet been addressed in a quantitative fashion. The latter is the central aim of the present work.

Our approach was inspired by the above-mentioned work of Thorpe and colleagues, who have shown that substrate analogues carrying either an oxa or a thia function at the *β*-position can undergo deprotonation (*16*). However, in these cases hydride transfer obviously cannot occur. The rate of formation of the postulated anionic ligand upon binding to MCADH is, unfortunately, too fast in these cases to be studied reliably [≥270 s^{-1} at 1 °C (*22*)], and the absorbance of the anionic species itself is obscured by that of the protein below 300 nm (*16, 22*). We have thus resorted to analogues that carry a *p*-substituted phenyl group at the acyl *β*-position of the CoA thioester. These have proven to possess some crucial advantages: the formation of the anionic species can be monitored directly by following its absorption, and the acidity of the αC−H can be modulated by the nature of the *p*-substituent. As will be shown, deprotonation of these analogues leads to intensely colored species, which allows the estimation of the pK_a of the bound species and thus of the corresponding pK_a shifts induced upon binding. We thus consider this reaction to mimic the stabilization of the anionic transition state and have thus named the ligands “chromogenic transition-state analogues”. Furthermore, the rates of deprotonation are sufficiently slow as to be accessible by stopped-flow measurements, thus permitting the assessment of deuterium isotope effects. A preliminary account of this work has been presented elsewhere (*23*).

MATERIALS AND METHODS

Materials. (*p*-Nitrophenyl)acetic acid *N*-hydroxysuccinimide ester, octanoyl-CoA, myristoyl-CoA, and 3′-dephospho-CoA were purchased from Sigma; coenzyme A (sodium salt) was from Pharma-Waldhof (D-40549 Düsseldorf-Oberkassel, Germany), (4-nitrophenyl)acetone was from Lancaster, and (4-aminophenyl)acetic acid was from Fluka. D_2O with a degree of deuteration not less than 99.8% was from Merck. Tributylphosphine, *N*,*N*′-dicyclohexylcarbodiimide, sodium acetylacetonate, and *N*-hydroxysuccinimide were from Aldrich.

Synthesis of p-Substituted Phenylacetones. (4-Cyanophenyl)acetone and (4-acetylphenyl)acetone were obtained from the corresponding *p*-substituted aryl bromides by a modification of the procedure by Sugai et al. (*24*). The aryl bromide, 10 mmol dissolved in 40 mL of dry DMF under N_2, was heated at 100 °C with 10 mmol of Cu(I) iodide and 50 mmol of sodium acetylacetonate to afford the corresponding (3-arylacetyl)acetonate [3 h for (4-cyanophenyl)acetone and 15 h for (4-acetylphenyl)acetone]. The formed product was subsequently deacetylated by addition of 40 mL of 1 M NaOH at ambient temperature and incubation for 3 h. After filtration and extraction with methylene chloride, the crude product was purified by silica gel flash chromatography (CH_2Cl_2/ethyl acetate 9:1) and identified by ^{1}H NMR and fast atom bombardment mass spectroscopy [(4-cyanophenyl)-acetone mp 51 °C, yield 35%; (4-acetylphenyl)acetone mp 34 °C, yield 45%).

Synthesis of the CoA Esters. *N*-Hydroxysuccinimide esters were synthesized according to Bellhof and Mutter *(25*) from the *p*-substituted phenylacetic acids. (4-Cyanophenyl)acetic acid was obtained as described by Jaeger and Robinson (*26*) starting from (4-aminophenyl)acetic acid. (4-Nitrophenyl)-acetyl-CoA (4NPA-CoA), (4-cyanophenyl)acetyl-CoA (4CN-PA-CoA), and (4-acetylphenyl)acetyl-CoA (4AcPA-CoA) were obtained by transesterification of the corresponding *N*-hydroxysuccinimide esters by a slight modification of the method described by Al-Arif and Blecher (*27*). One equivalent of CoASH dissolved in 100 mM $NaHCO_3$ pH 8.0 was added to tetrahydrofuran/H_2O (2/1), which contained tributylphosphine (2−3 equiv) to prevent oxidation. Upon addition of 8−10 equiv of the succinimide ester dissolved in tetrahydrofuran, the pH was adjusted with 5 N KOH to pH 7.9−8.1 and the conversion was followed by analytical HPLC. After consumption of the free CoASH, the mixture was acidified with 1 N HCl to pH ≈3 and extracted twice with diethyl ether (10 mL). The aqueous phase was neutralized (pH ≈6) with NaOH and lyophilized. The CoA esters were desalted over Waters Sep-Pak C18 Cartridges (35 mL volume) and purified by preparative HPLC using a Waters RCM (25 mm × 200 mm) Prep Nova Pak HR C18 column [50 mM NH_4HCO_3 pH 6.3 (buffer A) and 95% aqueous methanol (buffer B) with the following gradient: 0−5 min, 10% buffer B; 10 min, 20% buffer B; 40 min, 40% buffer B; 45−50 min, 100% buffer B; 55 min, 10% buffer B; flow rate 5 mL/min) with yields of 45−65%. For

analytical HPLC a Chromcart 25/4 Nucleosil C18 (5 μm) (Macherey-Nagel) column was used with the following gradient system: 5 mM KP_i, pH 6.0 (buffer A), and 95% MeOH (buffer B); 0−3 min, 10% buffer B; 3−43 min, 50% buffer B, 43−48 min, 100% (buffer B) 53−58 min, 10% buffer B. The following retention times at 30 °C were found: (4-acetylphenyl)acetic acid, 10.2 min; (4-cyanophenyl)acetic acid; 7.2 min; (4-nitrophenyl)acetic acid *N*-hydroxysuccinimide ester, 33.2 min; (4-cyanophenyl)acetic acid *N*-hydroxysuccinimide ester, 29.7 min; (4-acetylphenyl)acetic acid *N*-hydroxysuccinimide ester, 31.9 min; 4CNPA-CoA, 18.4 min; 4NPA-CoA, 19.2 min; 4AcPA-CoA, 19.5 min; (4-nitrophenyl)acetone, 28.7 min; (4-cyanophenyl)acetone, 26.2 min; and (4-acetylphenyl)acetone, 29.3 min. The CoA esters were identified by ^{1}H NMR and by their UV−visible spectra, which are characterized by a shoulder at $\lambda = 285$ nm ($OD_{260/285} \approx 2.2$). 3′-Dephospho-3S-C_8CoA was synthesized from 3′-dephospho-CoA and 3*S*-octanoate according to the method of Goldman and Vagelos (*28*) and purified over preparative HPLC. [2,2-$^2H_2$]-(*p*-nitrophenyl)acetyl-CoA was obtained by incubation of (*p*-nitrophenyl)acetyl-CoA at 4 °C in deuterated buffer at pH 8 for 24 h. The molar extinction coefficients were determined by the method of Ellman (*29*) using the *p*-nitrothiophenol anion absorbance ($\Delta\epsilon_{412} = 13\,600$ M^{-1} cm^{-1}): 4NPA-CoA, $\epsilon_{260} = 20\,800$ M^{-1} cm^{-1}; 4AcPA-CoA, $\epsilon_{253} = 28\,800$ M^{-1} cm^{-1}; 4CNPA-CoA, $\epsilon_{238} = 28\,150$ M^{-1} cm^{-1} and $\epsilon_{257} = 17\,390$ M^{-1} cm^{-1} (shoulder).

Miscellaneous. The growth of the *Escherichia coli* cells, strain BL 21, transformed with the plasmid containing the MCADH gene and the enzyme purification were as described by Kieweg et al. (*30*). LCADH was obtained as described elsewhere (*31*). MCADH and LCADH were routinely assayed in 50 mM KP_i buffer, pH 7.6, with octanoyl-CoA (100 μM) and with ferricenium hexafluorophosphate ($FcPF_6$) as electron acceptor (*32*). Only enzyme with an activity ≥1000 $FcPF_6$ min^{-1} was used. For MCADH $\epsilon_{446} = 14\,800$ M^{-1} cm^{-1} was used (*30*). Experiments as a function of pH were done in the following 50 mM buffers, all containing 250 mM KCl: Hepes for pH 6−7.5, Tricine for pH 7.5−8.5, Tris for pH 8.5−9, and glycine for pH 9−9.5. The pH was determined after each experiment in the reaction solution. For H_2O/D_2O mixtures the pH reading from the glass electrode was corrected as outlined in ref *33*. For the determination of the pK_as of the substituted acetonyl analogues, aliquots of ≈0.8 mM stock solutions were added to solutions of NaOH in H_2O (1 mM−5 M, pH 11−14.7) and the absorbance spectra were recorded as quickly as possible. UV−visible absorption spectra were obtained using a Kontron-Uvikon 920 spectrophotometer at 25 °C.

Rapid Reaction Studies. All experiments were carried out at 25 °C. Unless otherwise noted, the concentrations mentioned are those of the reagent after mixing, i.e., 1/1 dilution. For pH-dependent studies the enzyme was dissolved in the pH buffers described above that had twice the indicated final concentration. The solutions of the substrates were buffered only slightly with 10 mM KP_i, pH 6.0. The flow spectrophotometer has a thermostated 2 cm path length cell (*34*) and is equipped with a diode array detector (Spectroscopy Instruments GmbH, D-82205 Gilching) interfaced with a MacIntosh IIcx computer. Data were acquired using POSMA 2.3k software (Spectroscopy Instruments). Rapid reactions were routinely recorded in the range 300−650 nm using the "normal scan mode", which has a scan time of 10 ms/spectrum with a resolution of 2 pixels/nm. Experiments with 4NPA-CoA were recorded using a so-called "fast access" routine in which only selected wavelength (494.5−504.5 and 737−744.5 nm) were evaluated. For these experiments the normally used BG24A filter was removed in order to enhance the light intensity.

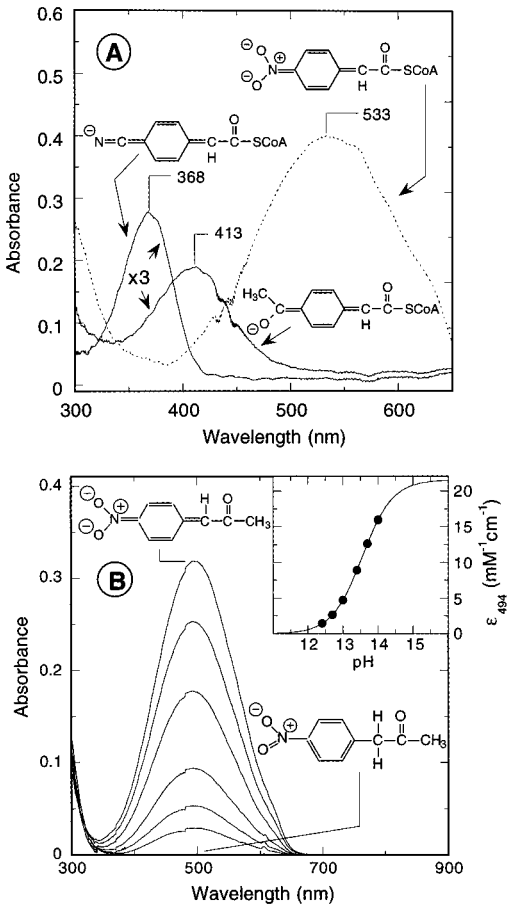

FIGURE 1: Absorbance spectra of 4-substituted phenylacyl chromophores and pH dependence. In panel A the spectra of the anionic forms of the acyl-CoA thioesters are displayed. 4NPA-CoA, 4CNPA-CoA, and 4AcPA-CoA, ≈25 μM (final concentration) in 5 mM KP_i, pH 6.0, were reacted with 0.5 N NaOH in the stopped-flow instrument at 25 °C (final pH ≈13.7). The traces shown are the first reliable ones, obtained within 10 ms upon mixing. All absorbance bands at $\lambda > 300$ nm disappear within 10 s due to hydrolysis of the thioester linkage. Due to this and to the variation in the determination of the time elapsed between end of flow and recording of the traces, the extinctions of the spectra shown have only qualitative character. For better comparison the absorption traces of 4CNPA-CoA and 4AcPA-CoA have been multiplied by a factor of 3. Panel B shows the pH dependence of the spectra of (4-nitrophenyl)acetone. (4-Nitrophenyl)acetone, 15 μL of a 1.33 mM stock solution in H_2O/MeOH (1:1), was diluted into 985 μL of aqueous NaOH (pH values 12.4, 12.7, 13.1, 13.4, 13.7, and 14, spectra from bottom to top). (4-Nitrophenyl)acetone in H_2O, pH < 11, is colorless. (Inset) Plot of ϵ_{494} versus pH. The line through the data points is the fit for a single ionization with pK_a =13.6, and an extrapolated ϵ_{494} ≈21 500 M^{-1} cm^{-1} for the fully ionized species.

Data Processing. For the static experiments, the absorbance changes were plotted against the ligand concentration and fitted to an appropriate equation such as described by Fersht (*35*). For the evaluation of kinetic experiments, the arithmetical mean of at least three kinetic traces was formed

Table 1: Spectral and Thermodynamic Properties of 4-Substituted Phenylacetyl-CoA, 3S-C_8-CoA, and 3′-Dephospho-3S-C_8-CoA Ligands and of Their Complexes with Human Wild-Type and E99G-MCADH and LCADH[a]

ligand structure	parameter	free ligand	MCADH complex	Glu99Gly-MCADH complex	LCADH complex
4NPA-CoA	pK_a (αC−H)	13.56[b]	4.9	5.2	nd
	λ_{max} (nm) anion, CT	533, −	497, 740	504, 730	≈497, 660
	$K_{d,app}$ (μM) at pH 7.6		≈25	≈25	≈170
	K_L (μM), extrapolated		(K_L, pH ≈6) 20	(K_L, pH < 4) 150	
			(K_L', pH > 10) 80	(K_L', pH > 7) 30	
4CNPA-CoA	pK_a (αC−H)	14.50[b]	nd	nd	nd
	λ_{max} (nm) anion, CT	368, −	376, 753	381, 742	
	$K_{d,app}$ (μM) at pH 7.6		≈46	≈17	≈240
4AcPA-CoA	pK_a (αC−H)	14.59[b]	nd	nd	np
	λ_{max} (nm) anion, CT	393, −	392, np	407, ≈780	
	$K_{d,app}$ (μM) at pH 7.6		≈153	≈60	≈200
3S-C_8CoA	pK_a (αC−H)	≈16.5[c]	5.2	nd	np
	λ_{max} (nm) anion, CT	<300, −	<300, 804	nd	<300, 660
	$K_{d,app}$ (μM) at pH 7.6		2	nd	≈13
	K_L (μM), extrapolated		(K_L, pH < 3) 25	nd	np
			(K_L', pH > 7) 2		
3′-dephospho-	pK_a (αC−H)	≈16.5[c,d]	6.15	nd	np
3S-C_8CoA	λ_{max} (nm) anion, CT	<300, −	<300, ≈805	nd	
	$K_{d,app}$ (μM), pH 7.6		2	nd	
	K_L (μM), extrapolated		(K_L, pH < 3) 3.5	nd	
			(K_L', pH > 7) 2		

[a] The extrapolated K_L values are those obtained from the fits to the data in Figures 5 and 6. nd, not determined; np, determination was not possible due to the instability of the enzyme under the particular conditions. [b] The values are those obtained using the corresponding acetonyl derivatives. [c] Values from ref *16*. [d] It is assumed that the absence of the 3′-phosphate does not affect this ionization.

and the resulting trace was fitted using program A (Dr. D. P. Ballou, University of Michigan). The dependence of velocities on the concentration was fitted to the equations described, e.g., by Strickland et al. (*36*), which are based on the assumption of a two-step equilibrium involving formation of a protein−ligand complex ($K_{2,1(L)} = k_2/k_1$), followed by a reversible reaction where both steps k_3 and k_4 are finite. The pH dependence of various parameters was fitted using the equations described by Fersht (*35*). With the exception of the analysis of rapid reaction traces, analyses were performed using appropriate fit routines and KaleidaGraph 3.0 for MacIntosh.

RESULTS

Physicochemical Properties of the Acyl-CoA Ligands. The main chemical feature of the chromogenic transition-state analogues selected for the present work is the presence of an acidic but kinetically stable αC−H bond combined with the absence of hydrogens in the β-position of the acyl chain. This precludes hydride transfer, and thus it is anticipated that αC−H deprotonation will yield a highly delocalized anion (cf. structures in Figure 1). In the case of 4NPA-CoA, deprotonation is in fact observed when the pH is raised above 13, by the formation of a transient red species, which disappears completely within seconds ($\tau_{1/2}$ ≈2 s in 0.5 N NaOH). It was thus of primary importance to determine the spectroscopic properties of the anionic species and the pK_a for αC−H deprotonation of the analogues used. Figure 1 panel A shows the spectra obtained upon mixing the acyl-CoA analogues with 0.5 M NaOH (final concentration) in the stopped-flow instrument. The anions are characterized by intense absorbancies in the near-UV−visible region, which are not present in the colorless neutral species. The above-mentioned instability, which is most likely attributed to hydrolysis of the thioester bond, precludes direct measurement of the pK_a values. To circumvent this dilemma we have thus resorted to the corresponding acetonyl model compounds in which the -COS-R functionality is replaced by -CO-CH_3 (cf. structure in Figure 1B). Recently Amyes and Richard (*8*) experimentally determined the pK_a value of the α-proton of ethyl thioacetate to be ≈21. This compares to a value of ≈19 for acetone (*37*) and indicates that the α-proton of thioesters is less acidic than that of ketones by ≈2 pK units. Thus, the determined pK_a values for the *p*-substituted phenylacetones can be taken as a lower estimate of those of the corresponding CoA analogues. Figure 1 panel B shows the pH dependence of the spectra of *p*NO_2-phenylacetone; the estimated pK_a is 13.6 (extrapolated $\epsilon_{494,\ anion}$ ≈21 500 M^{-1} cm^{-1} at pH > 16). Slightly higher pK_a values of ≈14.5 and ≈14.6 were found for (*p*-cyanophenyl)acetone and (*p*-acetylphenyl)acetone. The absorbance properties and pK_a values of the analogues are listed in Table 1. The λ_{max} values of the anionic species are strongly dependent on the solvent. Thus, compared to aqueous solution, *p*NO_2-phenylacetonate in methanol and acetonitrile exhibits a red shift to λ_{max} ≈500 and ≈540 nm, respectively (not shown). This property is useful for assessing the polarity at the locus of binding.

Reactions with the Enzyme: Formation of Colored Complexes in Static Experiments. Upon addition of 4NPA-CoA to MCADH large changes in the visible absorption spectrum of the latter occur, which are proportional to the concentration of the ligand and show saturation behavior (Figure 2). The absorbance in the 450−520 nm region is approximately doubled at saturation and the λ_{max} is shifted toward λ = 466 nm. In addition a new long-wavelength band with λ_{max} ≈740 nm is formed. The absorbance increase at 450−500 nm is attributed mainly to formation of anionic, enzyme-bound 4NPA-CoA with some contribution from the perturbation of the flavin chromophore. The long-wavelength band is

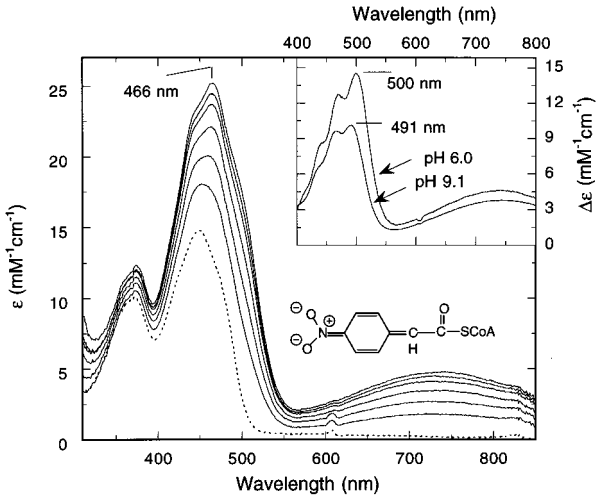

FIGURE 2: Spectral changes upon titration of MCADH with 4NPA-CoA. The lowest trace (•••) is the spectrum of MCADH, 8.24 μM in 50 mM Hepes and 250 mM KCl, pH 6.0, $T = 25$ °C. Subsequent traces in ascending order are obtained upon addition of 1.04, 2.07, 4.14, 8.26, 14.0 and 39.4 equiv of 4NPA-CoA. All spectra were recorded versus an equal concentration of ligand in the reference cuvette and are corrected for dilution. The inset shows difference spectra for complexed minus uncomplexed enzyme extrapolated to full complexation, at 25 °C and at the pH values indicated. The absorption band that forms at $\lambda \approx 490-500$ nm is that of anionic 4NPA-CoA, and that with a $\lambda_{max} \approx 740$ nm results from the charge-transfer interaction between the 4NPA-CoA anion and the oxidized flavin.

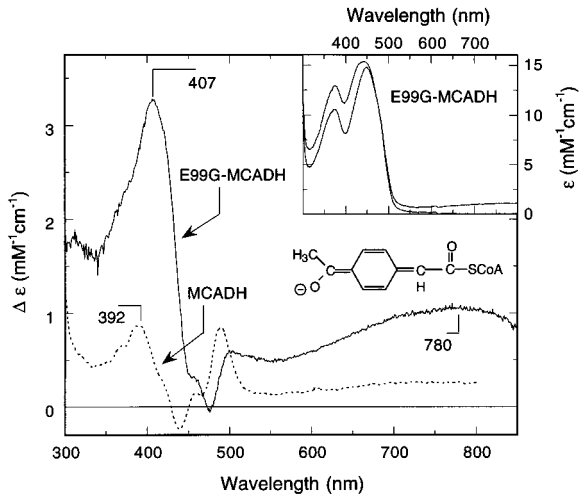

FIGURE 3: Spectral changes accompanying binding of 4AcPA-CoA to MCADH and Glu99Gly-MCADH. Conditions: [MCADH] = 12.0 μM, [Glu99Gly-MCADH] = 10.3 μM, 50 mM KP_i, pH 7.6, $T = 25$ °C. Main figure: Difference spectra between fully complexed and uncomplexed forms of MCADH (•••) and Glu99Gly-MCADH (—). The inset shows a comparison of the spectra of uncomplexed Glu99Gly-MCADH and the Glu99Gly-MCADH∼4AcPA-CoA (anion) complex (lower and upper traces, respectively).

attributed to a charge-transfer absorption between the same anion and the oxidized flavin. This is illustrated by the difference spectra shown in the inset of Figure 2, which also document the effect of pH on the spectra. Note the larger extent of anion formation occurring at pH 6 compared to pH 9.

There are marked differences in the interaction of 4NPA-CoA as compared to *p*-CN- and *p*-$COCH_3$-phenylacetyl-CoA: with the latter, there appears to be very little if any formation of the anionic species, as can be deduced by the absence of absorption attributable to its anionic form in the 400 nm area and in the charge-transfer region (Figure 3). To understand the peculiar pH effect, we have used Glu99Gly-MCADH (*38*). Glu99 flanks the bottom of the active-site cavity of MCADH with its -COOH group at a distance where it could interact with ligands (cf. below). Indeed with Glu99Gly-MCADH, both *p*-CN- and *p*-CH_3-CO-PA-CoA do form appreciable amounts of their anions upon binding. The difference spectra (complexed *minus* uncomplexed enzyme) obtained with *p*-CH_3-CO-PA-CoA and hwt-, or Glu99-Gly-MCADH are significantly different in the 500 nm region (Figure 3). We attribute this to the difference in charge: Binding of ligands carrying a neutral acyl substituent to MCADH induces a positive (difference) absorption in this spectral area (*39*, *15*, *16*), thus *p*-CH_3-CO-PA-CoA is in its neutral form with hwtMCADH. On the other hand, the negative difference observed with Glu99Gly-MCADH, depicted in Figure 3, is consistent with the presence of anionic ligand in the complex.

With *p*-CN-phenylacetyl-CoA, full deprotonation appears to occur both with hwtMCADH (not shown) and with the Glu99Gly mutant (Figure 4). In this case the absorbance of the anionic, enzyme bound ligand is red-shifted by ≈10 nm compared to that of the free species (Figure 1), as opposed

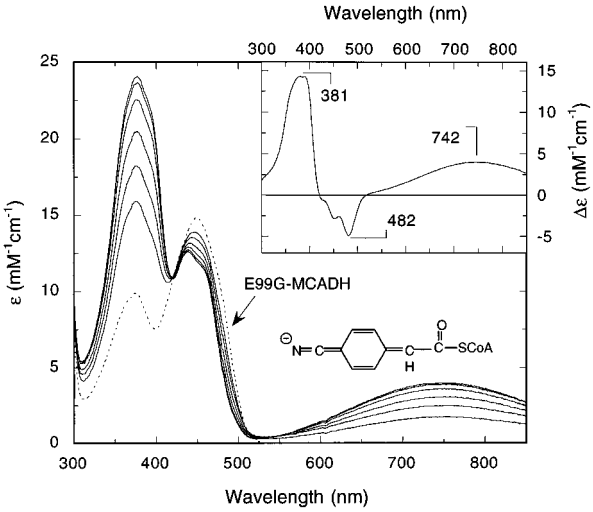

FIGURE 4: Reaction of Glu99Gly-MCADH with 4CNPA-CoA. The spectrum of Glu99Gly-MCADH, 11.24 μM, in 50 mM KP_i, pH 7.6, and at 25 °C is depicted by the dotted (•••) trace. Upon addition of 0.96, 1.91, 3.81, 8.52, 17.77, and 26.80 equiv of 4CNPA-CoA, the traces in the ascending order (at 400 and 750 nm) are obtained. The inset shows the difference spectrum between fully complexed and uncomplexed enzyme. Note that the band with $\lambda_{max} = 381$ nm is due to the anionic ligand (see structure), and that centered around $\lambda \approx 750$ nm is due to the CT interaction of the latter with the oxidized flavin.

to the case of 4NPA-CoA, where a ≈30 nm hypsochromic shift is observed. Again the perturbation of the flavin lowest energy transition has a negative difference spectrum in the 500 nm area, consistent with the interaction with a negatively charged species (Figure 4, insert). The spectroscopic and physical properties of the complexes at different pH values are listed in Table 1.

Analogous experiments with the same ligands were carried out also with LCADH, in which there is no charged group corresponding to Glu99 in MCADH (*30*). Surprisingly, while binding can be monitored by the typical perturbation of the oxidized flavin spectrum, with 4CNPA-CoA, and

4AcPA-CoA there are no effects suggesting ligand (an)-ionization. With 4NPA-CoA, a small absorbance increase in the 500 nm region ($\epsilon_{497} \approx 2.3$ mM^{-1} cm^{-1}) and a very weak long-wavelength band ($\epsilon_{740} \approx 0.3$ mM^{-1} cm^{-1}) suggest formation of ligand anion and of the corresponding CT complex. The extent of anion formation increases with pH (not shown), similar to the observations made with Glu99Gly-MCADH, but never exceeds 15% of the amount of bound anion observed with MCADH. The K_Ls for L−H binding to LCADH (Table 1) are about 1 order of magnitude higher than those for MCADH.

pH Effects on the Binding of 4NPA-CoA. Figure 5 panel A shows the pH dependence of the maximally attainable, apparent extinction coefficient ϵ_{CT} in the charge-transfer region. The data were obtained from titration experiments such as that shown in Figure 2. With 4NPA-CoA and MCADH, the absorbance changes due to anion formation are maximal at pH 6−6.5; at pH < 6 the absorbance decreases toward zero and reflects an apparent p$K_{a,1} \approx 5$. The pH dependence cannot be measured reliably at pH < 5 due to the instability of the enzyme. At pH > 6 a decrease of ϵ_{CT} is followed by a plateau and the behavior reflects an apparent p$K_{a,2} \approx 7.3$. The fit of the data shown in Figure 5A also yields an estimate of the apparent ϵ_{CT} of the two species linked by the equilibrium governed by p$K_{a,2}$. They are $\epsilon_{CT1} \approx 5200$ M^{-1} cm^{-1}; $\epsilon_{CT2} \approx 3800$ M^{-1} cm^{-1}; ϵ_{CT} for the species at pH < p$K_{a,1}$ was assumed to be = 0 M^{-1} cm^{-1}, and $\epsilon_{CT-E99G} \approx 6800$ M^{-1} cm^{-1}. When the absorbance changes at $\lambda \approx 500$ nm are used for similar plots, the same pK_as are obtained, and the relative difference between the corresponding, estimated $\epsilon_{500,1}$ and $\epsilon_{500,2}$ values is larger. In contrast to the two pK_a values found with MCADH, only one p$K_a \approx 5.2$ is observable with the Glu99Gly mutant (Figure 5A). It is noteworthy that, qualitatively, the same behavior is observed with MCADH using 3S-C_8CoA as the ligand (compare to Figure 6A).

The pH dependence of the pK_ds for binding of 4NPA-CoA to MCADH and to the Glu99Gly mutant are plotted according to Dixon (*40*) in Figure 5B. While at pH < 6.5 both MCADH and the E99G mutant exhibit a similar behavior, at pH > 7 only MCADH shows an increase of the apparent K_d. This is consistent with the effect being due to the ionization of Glu99-COOH, i.e., the weaker binding with native MCADH at pH > p$K \approx 7.3$ resulting from the repulsion of the charges of Glu99-COO$^-$ and of 4NPA-CoA$^-$. The theoretical titration curves were generated using the Dixon equation:

$$\mathrm{p}K = -\log K_L + \log\left(1 + \frac{K_{EL1}}{[H^+]}\right) - \log\left(1 + \frac{K_{E1}}{[H^+]}\right) - \log\left(1 + \frac{K_{E2}}{[H^+]}\right) + \log\left(1 + \frac{K_{EL2}}{[H^+]}\right) \quad (1)$$

where K_L is the dissociation constant of neutral ligand (L−H) from the neutral form of the enzyme E−H. According to the rules of Dixon (*40, 41*), pK_{EL1} and pK_{EL2} are ionizations of the enzyme−ligand complex (E∼L−H) and pK_{E1} and pK_{E2} are ionizations of uncomplexed enzyme (or ligand). (See also Table 1 for values.) For the simulation pK_{EL1} was fixed as 5.2, i.e., the pK observed for the formation of anionic 4NPA-CoA in the E∼L complex and obtained from the plots of Figure 5A; pK_{E2} was similarly taken as 7.3, i.e., the apparent pK for ϵ_{CT} formation derived from the same plot (Figure 5A). The (apparent) p$K_{E1} \approx 6$ and p$K_{EL2} \approx 8$ are the values resulting from the fit of the data points in Figure 5B. Use of the extended equation for mutually affecting ionizations (*41*) did not improve the simulation. For E99G-MCADH, only the pK_{E1} and pK_{EL1} terms of eq 1 were required for generating the curve fits.

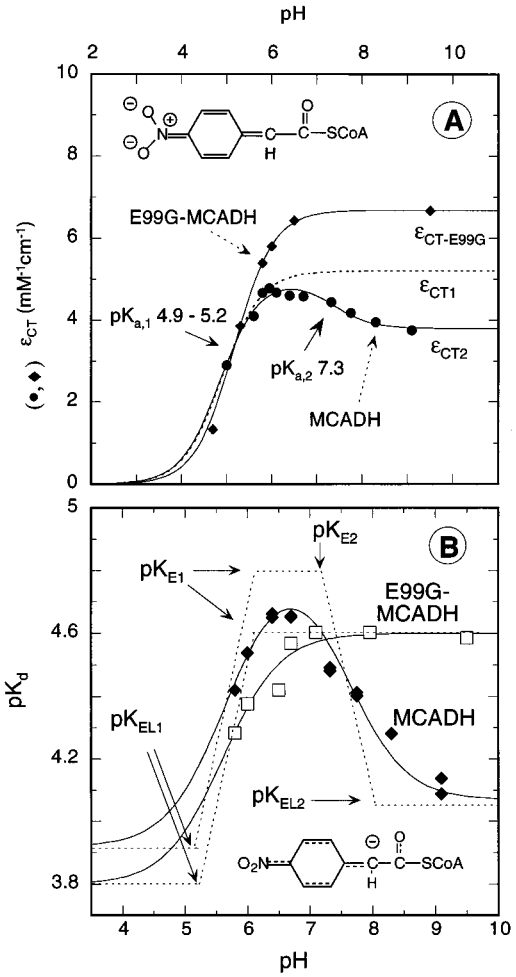

FIGURE 5: pH dependence of the interaction of 4NPA-CoA with MCADH and Glu99Gly-MCADH. (A) Interactions with 4NPA-CoA. The data points (●, ◆) are the extrapolated ϵ_{CT} values (λ = 740 nm for MCADH and λ = 735 nm for Glu99Gly-MCADH) obtained from titrations as described in Figure 2 at the pH values indicated (buffer systems detailed in Materials and Methods). At pH < 5.5, titrations could not be carried out due to the instability of the proteins; in this case the extent of ligand anion formation was estimated by addition of an excess (660 μM) of 4NPA-CoA to enzyme at concentrations ranging from 13.5 to 15 μM. The solid lines through the data points are for fits to one or two ionizations, as appropriate; the dotted line shows dependence of the effects for MCADH calculated for a hypothetical case in which pK_2 is absent (and using p$K_{a,1}$ = 4.9 and ϵ_{CT1} = 5200). The extinctions of the complexes at pH < 3 were set constant at 0. (●) MCADH; (◆) Glu99Gly-MCADH. ϵ_{CT} are the extinction coefficients estimated for high pH. (B) pH dependence of p$K_{d,app}$ for binding of 4NPA-CoA to MCADH (◆) and Glu99Gly-MCADH (□) plotted according to Dixon (*40*). The segments (···) have slopes = 0 or 1. The curves were generated using eq 1 and, for MCADH, pK_L = 3.9, pK_1 = 5.2, pK_2 = 6.0, pK_3 = 7.3, and pK_4 = 8.0; for Glu99Gly-MCADH, pK_L = 3.8, pK_1 = 5.2, and pK_2 = 6.0. See text for further explanations.

pH Effects on the Binding of 3S-C_8CoA and 3′-Dephospho-3S-C_8-CoA. The effects observed with these ligands and

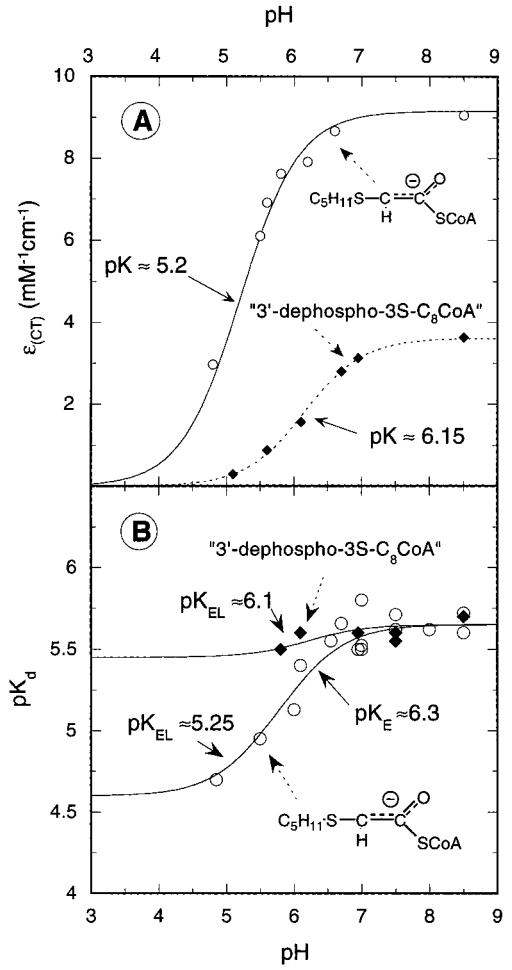

FIGURE 6: pH dependence of the interaction of 3S-C_8CoA and 3′-dephospho-3S-C_8CoA with MCADH. (A) pH dependence of the spectral effects induced upon binding of the two ligands. The curves are the best fits for one ionization. The data points at pH > 5.5 are the extrapolated $\epsilon_{811\ nm}$ values for the fully complexed enzyme obtained from titration experiments, and those at pH = 4.8 and 5.5 were obtained by addition of excess (80 μM) 3S-C_8CoA to 12 μM MCADH. For the titrations at pH > 5.5, 10 cm cuvettes were used. (B) pH dependence of p$K_{d,app}$ for binding of 3S-C_8CoA (○) and 3′-dephospho-3S-C_8CoA (◆) to MCADH, plotted according to Dixon (*40*, *41*). The curves were generated using eq 1 and, for 3S-C_8CoA, pK_L = 4.6, pK_1 = 5.25, and pK_2 = 6.3; for 3′-dephospho-3S-C_8CoA, pK_L = 5.45, pK_1 = 6.1, and pK_2 = 6.3. See text for further explanations.

MCADH are shown in Figure 6A. They resemble those of 4NPA-CoA with E99G-MCADH described above (cf. Figure 5A). This indicates that the ionization of Glu99-COOH only affects that of the ligand αC−H when the resulting charge can delocalize beyond C(3) of the ligand chain. The same type of spectral changes as with 3S-C_8CoA (*16*) occur upon binding of 3′-dephospho-3S-C_8CoA (not shown), albeit with lower ϵ_{CT} values. The behavior of this ligand, in which the adenosine 3′-phosphate group with a pK ≈6.5 (*42*) is absent, was studied in order to differentiate whether the pK_{E1} ≈6 (cf. above) is an ionization of (free) enzyme or of (uncomplexed) ligand. The (apparent) pKs reflected by the spectral changes occurring upon binding of 3S-C8CoA and 3′-dephospho-3S-C_8CoA are ≈5.2; and ≈6.15, respectively (Figure 6A). As with 4NPA-CoA, they are attributed to the ionization of enzyme-bound ligand. The higher pK observed with the 3′-dephospho analogue suggests a less optimal binding of the latter, resulting in an inferior stabilization of the anion.

The pH dependence of the apparent K_d for binding of these ligands is plotted according to Dixon (*40*) in Figure 6B. Reasonable simulations of the observed pK_d vs pH data for binding of both ligands are obtained using pK_{EL} = 5.2 and 6.1, i.e., the values obtained from the plots of Figure 6A, and the same value of pK_E = 6.3 for both ligands. The values for the estimated dissociation constants K_L at the pH extremes are also listed in Table 1. According to the Dixon rules (*40*, *41*) and in analogy to the case of 4NPA-CoA, the apparent pKs are assigned as indicated on Figure 6B. pK_E = 6.3 thus corresponds to the pK ≈6 derived similarly from the pH dependence of binding of 4NPA-CoA (Figure 5B). The apparent K_d for binding of the 3′-dephospho analogue shows little effect on pH (Figure 6B), it has the same value as that of 3S-C_8CoA at pH > pK_{EL} ≈5.2, indicating that the 3′-phosphate as such does not affect binding. Its pK_d vs pH behavior, i.e., the absence of an apparent pH dependence, is readily explained by the coincidences of pK_{EL} ≈6.1 and pK_E ≈6.3. If the second ionization were to be absent with the 3′-dephospho ligand, an increase of pK_d vs pH at pH > 6.1 with a slope = 1 should be observed at pH > pK_{EL} ≈6.1 (*40*, *41*). On the basis of these considerations the apparent pK ≈6−6.3 is attributed to an ionization of uncomplexed enzyme as opposed to one of free ligand.

Kinetics of Enzyme Interaction with the Ligands: (A) [α-$^2H_2$]-4NPA-CoA and Solvent Isotope Effects. [α-$^2H_2$]-4NPA-CoA was used for a kinetic verification, via measurement of a deuterium isotope effect, of the assumption that the observed spectral changes are directly connected with the abstraction of the ligand αC−H. Incubation of 4NPA-CoA in D_2O buffered with 10 mM NaP_i, pD 7.1, leads to >90% exchange of the αC−H with deuterium within 20 min, as can be verified by ^{1}H NMR spectroscopy (data not shown). While this rate is insignificant compared to the enzyme-catalyzed rate of deprotonation, it does not allow experimentation with deuterated substrate in H_2O due to the time required for sample preparation. We have thus estimated the isotope effect by studying the reaction in a 50% mixture of buffered D_2O/H_2O (10 mM sodium phosphate, pD 7.1). For this purpose, enzyme and [α-$^2H_2$]-4NPA-CoA were dissolved in H_2O and D_2O, respectively, and the two solutions were mixed in the stopped-flow instrument. To discriminate between the primary isotope effects and solvent isotope effects, the solvent isotope effect was determined by studying the rate of reduction of MCADH with myristoyl-CoA in D_2O/H_2O mixtures ranging from 0% to 50% D_2O. The rate of enzyme flavin reduction is 6.1 s^{-1} in pure H_2O and 5.5 s^{-1}, i.e., ≈90%, in 50% D_2O, and the dependence on the D_2O fraction is linear (not shown). From this a rate ≈5.0 s^{-1} can be extrapolated for 100% D_2O (at a constant [myristoyl-CoA] = 100 μM). Thus the rates measured with [α-$^2H_2$]-4NPA-CoA in 50% D_2O and used to estimate the intrinsic primary isotope effects (cf. below) have been corrected by the factor 1.1.

(B) Reaction of 4NPA-CoA with MCADH. The time course for the spectral changes occurring upon mixing 4NPA-CoA with normal enzyme is essentially monophasic—it has the same rate at 495 and 720 nm (Figure 7)—and the reaction is complete within 200 ms. The plots of k_{app} versus [4NPA-CoA] shown in Figure 8 exhibit the dependence typical of a process in which binding is followed by a reversible event leading to an equilibrium as described in eq 2 (E is oxidized

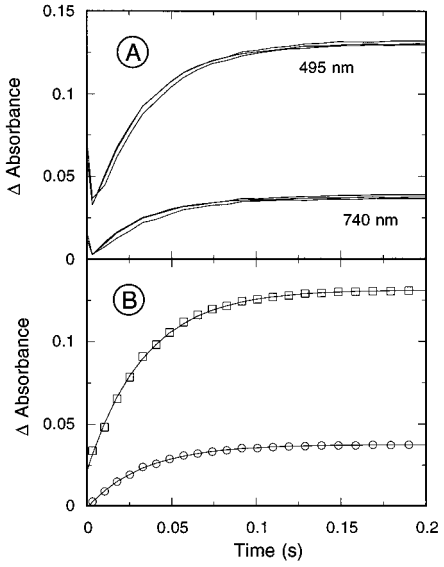

FIGURE 7: Time course of the reaction of 4NPA-CoA with MCADH. (A) Three typical kinetic traces at two wavelengths showing spectral changes occurring upon mixing 4NPA-CoA with MCADH in the stopped-flow instrument. Conditions: [MCADH] = 6.2 μM in 50 mM Tricine buffer, pH 7.5, containing 250 mM KCl; [4NPA-CoA] = 700 μM in 5 mM KP_i, pH 6.0, at 25 °C (final concentrations). (B) The arithmetic means of the traces shown in panel A are represented by (○) and (□) for changes at λ = 740 and 495 nm. The lines through the points are for single-exponential fits with estimated rates of 29.3 and 29.9 s^{-1} at λ = 495 and 740 nm, respectively.

MCADH, L−H is phenylacetyl-CoA ligand, $K_{2,1(L-H)}' = k_2/k_1$, binding step, and k_3 and k_4 represent de- and reprotonation of bound ligand):

$$E + L{-}H \underset{k_2}{\overset{k_1}{\rightleftharpoons}} E{\sim}L{-}H \underset{k_4}{\overset{k_3}{\rightleftharpoons}} E{\sim}L^{-} \qquad (2)$$

This type of behavior has been analyzed in extenso by Strickland et al. (*36*) and is characterized by an abscissa intercept of k_{app} at [L−H] ⇒ 0, which corresponds to step k_4 in eq 2 and by a $k_{app} = k_3 + k_4$ at [L−H] ⇒ ∞. By this analysis, values for $K_{2,1(L-H)}$, k_3, and k_4 for the [α-^{1}H] and [α-^{2}H] forms of 4NPA-CoA were obtained between pH 6.5 and 9.5 (Table 2); the corresponding isotope effects are also listed in Table 2.

The kinetics of binding of 4NPA-CoA to the Glu99Gly mutant were measured at pH 7.6. Overall, the behavior is similar to that observed with MCADH; however, the time course of the reaction is somewhat biphasic (not shown). The first, fast phase accounts for 90−98% of the total observed changes. Its apparent rate k_{app} obtained by extrapolation to [L−H] ⇒ ∞ is approximately 3-fold (150 ± 10 s^{-1}) that found with MCADH (Table 2) and the apparent $K_{2,1(L-H)}$ ≈70 μM, is ≈$^1/_{10}$ of what is found for MCADH (see below). This is consistent with the assumption that the active-center cavity of E99G-MCADH can better accommodate the *p*NO_2-phenyl-residue compared to MCADH. As with MCADH, with the mutant ligand deprotonation (k_3) is reversible, i.e., k_4 (cf. eq *2*) has a finite value as deduced from data analysis according to Strickland et al. (*36*) (not shown). Thus a rate k_4 ≈20 (± 10) s^{-1} is obtained, which, subtracted from k_{app} = 150 s^{-1}, yields an estimated value for k_3 ≈130 s^{-1}. The second, slow phase might reflect secondary processes and was not included in the analysis. From these data it is concluded that the interaction of 4NPA-CoA with E99G-MCADH is essentially of the same type as with MCADH.

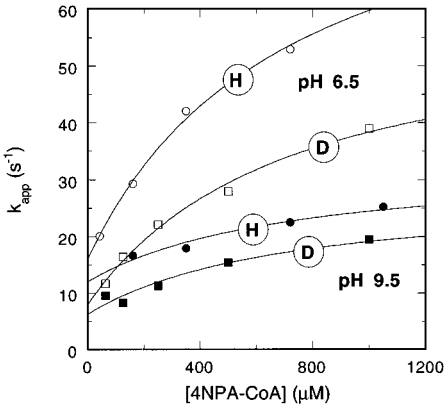

FIGURE 8: Rates and concentration dependence for reaction of [α-^{1}H]-4NPA-CoA and [α-^{2}H]-4NPA-CoA with MCADH at pH 6.5 and 9.5. Conditions were as described in the caption to Figure 7, with the exception of the use of varying buffer systems at different pH values (see Materials and Methods). The [4NPA-CoA] was in the range 45−1000 μM (final concentrations). k_{app} is the velocity estimated from experiments such as those shown in Figure 7. In the case of [α-^{2}H]-4NPA-CoA, the experiments were carried out by mixing MCADH in H_2O, with [α-^{2}H]-4NPA-CoA dissolved in 100% ^2H_2O. The corresponding values are corrected for the deuterium solvent isotope effect (factor 1.1; see text for details). The solid lines represent the best fits obtained using the method reported by Strickland et al. (*36*).

Table 2: Kinetic Parameters and Isotope Effects for the Reaction of 4NPA-CoA with MCADH[a]

	pH				
parameter	<6.5	6.5	7.5	9.5	>9.5
k_3 [α-^{1}H]-	76 ± 5	75 ± 3	55 ± 1	21 ± 3	19 ± 3
k_3 [α-^{2}H]-	53 ± 5	52 ± 3	41 ± 2	22 ± 3	18 ± 3
H/D	*1.43*	*1.44*	*1.34*	*≈1*	*≈1*
k_4 [α-^{1}H]-		16 ± 1	11 ± 0.2	12 ± 1	
k_4 [α-^{2}H]-		8 ± 1	6 ± 1	6 ± 1	
H/D		*2*	*1.8*	*2*	

[a] The values for [α-^{2}H]-4NPA-CoA are corrected for the solvent isotope effect; those at pH < 6.5 and pH > 9.5 are extrapolated values obtained from the plots of Figure 9. See text for further details.

It should be pointed out that, with 4NPA-CoA and MCADH, due to the high $K_{2,1(L-H)}$, saturation with 4NPA-CoA could not be attained (cf. Figure 8); this leads to a relatively high error in the estimation of $K_{2,1(L-H)}$. The most reliable results (710 ± 200 μM) were obtained using [α-^{1}H]-4NPA-CoA and at pH 6.9. For the majority of the other sets of data at various pH values, and as shown in Figure 9A, for $K_{2,1(L-H)}$, only an average value ≈710 ± 200 μM can thus be estimated. A pH dependence is not apparent; if occurring, its magnitude is probably smaller than the data scatter. For the estimation of the majority of the values of k_3 and k_4 at the various pH values, using fitting routines and the approach shown in Figure 8, $K_{2,1(L-H)}$ was thus held constant at 700 μM. From Figure 8 it is apparent that the magnitude of both steps k_3 and k_4 depends on the pH. The full dependence of these values on pH is depicted in Figure 9B, from which an apparent p*K* value of ≈7.8 can be estimated for k_3. For k_4, no significant pH dependence is appar-

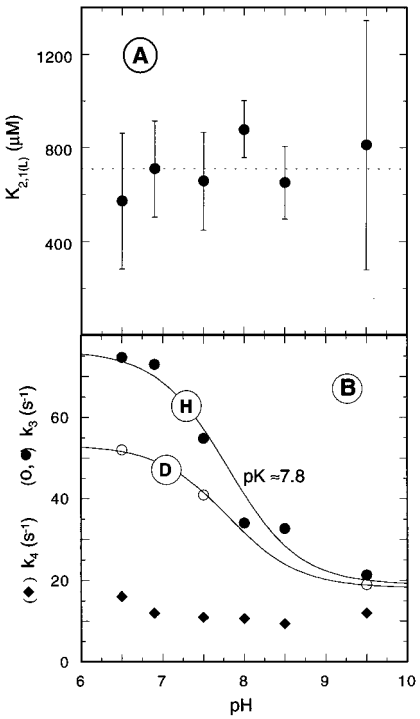

FIGURE 9: pH dependence of the kinetic parameters obtained for the reaction of 4NPA-CoA with MCADH obtained from stopped-flow experiments. (A) Dependence of $K_{2,1(L-H)}$, the dissociation constant for 4NPA-CoA. (B) Dependence of the rates k_3 and k_4. Conditions were as described in the caption to Figure 7. The lines through the data points are the fits obtained using the pH equation. In the case of the deuterated substrates the fit was obtained using the same pK values as found for the [α-^{1}H] substrates.

ent. The data reported in Table 2 for [α-$^2H_2$]-4NPA-CoA are corrected for the solvent deuterium isotope effect of ≈1.1 as explained above. Thus we consider the isotope effects found at pH 6.5 and 7.5 (Table 2) as primary ones. Consequently the spectral species described above can be attributed to the product resulting from fission of the αC−H bond, i.e., anionic 4NPA-CoA and its complex with oxidized MCADH. Interestingly, the deuterium isotope effect on k_3 disappears at high pH while that on k_4 remains fairly constant (Table 2). An interpretation of this finding has not been attempted, since at high pH exchange reactions both at the αC−H and involving active-site residues are probably relevant.

DISCUSSION

Formation of Anionic Ligands upon Binding to MCADH. The first salient point emerging from the present data is the presence of the (an)ionized forms of the *p*-substituted phenylacetyl-CoA ligands at the active center of MCADH. This can be deduced unequivocally from the spectral effects occurring upon binding, in particular from the direct observation of the absorption of the ionized ligand (compare Figures 2−4 with Figure 1A) and from the occurrence of a primary deuterium isotope effect on αC−H on the kinetics of formation of these species. This justifies the concept that this type of ligand can generate analogues of the transition state occurring during α,β-dehydrogenation. This analogy is shown in Scheme 1, in which structures A and B represent the events initiating catalysis with substrate, and C and D represent abstraction of H^+ from the ligand αC−H.

From previous studies it has been concluded (*6*) that the fissions of the substrate αC−H and βC−H bonds occur

Scheme 1: Comparison of the Interactions of Normal Substrate (Left-Hand Side) and of 4NPA-CoA (Right-Hand Side) with Active-Center Functional Groups[a]

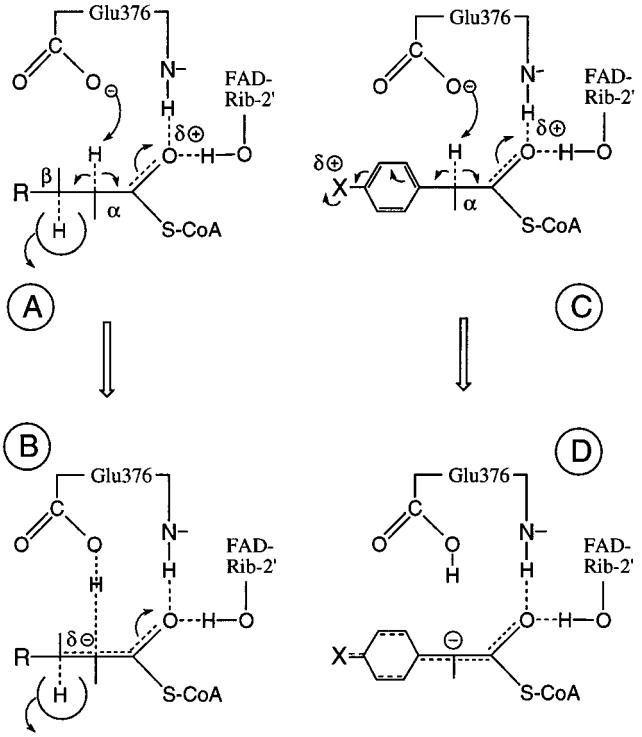

[a] The H-bonds with the thioester carbonyl activate the αC−H function (A, C). In the case of 4NPA-CoA, the anion formed (D) cannot react further and is stabilized by delocalization into the aromatic ring system and into the thioester carbonyl. With substrate, cleavage of the αC−H and βC−H bonds is concerted (*5*); however, deprotonation precedes the expulsion of βC−H as hydride, generating a partial negative charge (B), which delocalizes toward the activated carbonyl. See text for further details.

concertedly, as opposed to via definite intermediates such as the (delocalized) substrate α-carbanion. This was derived from the observation that the (single) deuterium isotope effects (k_H/k_D) on αC−H (k_H/k_D ≈2.5) and on βC−H bond cleavage (k_H/k_D ≈14) behave multiplicatively when αC-(^{2}H)βC(^{2}H) substrate is dehydrogenated (k_H/k_D ≈28) (*6*). The seeming contradiction of the occurrence of a carbanionic intermediate versus that of a concerted reaction can be circumvented by assuming that in the transition state bond cleavage of the αC−H precedes that of the βC−H; i.e., that a partial negative charge develops on the α-carbon and that the reaction profile is asymmetric as shown in Scheme 1B. Such an asymmetry is consistent also with the magnitude of the primary isotope effects mentioned above. The small effect on αC−H corresponds to a large amount of cleavage of this bond in the transition state, while the very large one on βC−H reflects a more symmetrical profile for transfer of βH to the flavin. This is also in accordance with the concept that a crucial factor in α,β-dehydrogenation catalysis is the acidification of the αC−H due to specific interactions with the thioester carbonyl function (*9, 43, 44*). In the case of the analogues the negative charge formed is stabilized by delocalization as shown by structure D.

Assignment of Apparent pKs to Functional Groups. The interpretation of the pH dependencies shown in Figures 5 and 6 is of primary importance for further discussion. From the spectral effects observed upon binding of 4NPA-CoA to

Scheme 2: Steps Involved in the Reaction of Ligand L−H to MCADH or to Glu99Gly-MCADH[a]

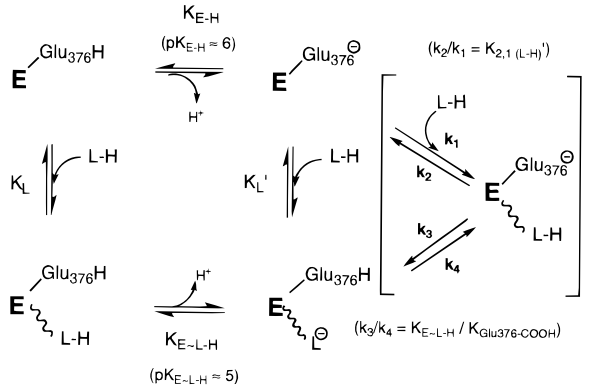

[a] With MCADH, L−H = 3S-C_8CoA; with Glu99Gly-MCADH, L−H = 4NPA-CoA; see also Figure 5. K_L represents simple binding to enzyme in which Glu376 is neutral. K_L' is binding to the form in which Glu376 is ionized; it includes concomitant transfer of H^+ from L−H to Glu376-COO^-. $K_{E\sim L-H}$ and $K_{Glu376-COOH}$ are the microscopic pKs for the ionizations of L−H and Glu376-COOH in the complex. The section in brackets shows the subdivision of step K_L' into a binding step $K_{2,1(L-H)}'$ followed by exchange of H^+. The data for this latter section were obtained with stopped-flow experiments. See text for further details.

wild-type MCADH between pH 5 and 9, two pK values at ≈5.1 and ≈7.3 were identified. When Glu99-COOH, which is located in the substrate binding pocket, is removed by mutagenesis (E99G-MCADH) the "second" pK_a ≈7.3 is absent. This ionization is therefore attributed to Glu99-COOH, and according to the Dixon rules, this pK is an ionization of an uncomplexed species (*40*, *41*). The fact that on binding of 3S-C_8CoA to MCADH this pK ≈7.3 is not observed (Figure 5B) can be explained using available structural data and will be addressed below. For the cases of MCADH/3S-C_8CoA and 4NPA-CoA/E99G-MCADH, which exhibit only one detectable pK value, the results can be discussed on the basis of Scheme 2. There, the leftmost segment (and K_L) represents binding of neutral ligand L−H to enzyme in which Glu376 is protonated (E∼Glu376-COOH). The central and right-hand side depict binding to the corresponding deprotonated form of the enzyme (E∼Glu376-COO^-, K_L'). The value of K_L (Table 1) is obtained from the fits depicted in Figure 5B or 6B by extrapolation to pH < pK. On the basis of two straightforward arguments, we assign the pK_a 4.9−5.2 to enzyme-bound ligand (E∼L−H) (lower branch in Scheme 2): First, from the formation of absorption of anionic ligand (λ ≈490−500 and ≈380 nm for 4NPA-CoA and 4CNPA-CoA, Figures 2 and 4) *and* that of the CT interaction, the ionization must involve bound ligand. Second, the upward curvature in the Dixon-type plots corresponding to pK ≈5 (Figures 5B and 6B) requires this ionization to be associated with a *bound* species, i.e., with either an enzyme functional group or with ligand L−H in their complex (E−H∼L−H) (*40*, *41*). The finding of similar apparent pKs ≈5 for 4NPA-CoA (Figure 5) and 3S-C_8CoA (Figure 6) is probably coincidental since with 3′-dephospho-3S-C_8CoA the corresponding pK is shifted to ≈6.1 (Figure 6).

The next ionization that can be derived from the plots of Figures 5B and 6B is the apparent pK_a ≈6.3, which again according to the Dixon rules belongs to a free species, thus to either E−H or L−H. Clearly, ionization of the free ligand αC−H has a much higher value around 13.6−16. The ionization of free CoA 3′-phosphate (pK ≈6.5) can be ruled out on the basis of the experiments with 3′-dephospho-3S-C_8CoA. We therefore assign this pK_a ≈6.3 to a function in uncomplexed enzyme. From the concatenation of thermodynamic parameters as shown in Scheme 2 it appears logical that this group is Glu376-COOH. While the arguments just discussed cannot exclude rigorously other alternatives, this crucial interpretation is fully supported by results obtained with the Glu376His mutant of MCADH (Kieweg and Ghisla, unpublished results). The latter is competent in substrate dehydrogenation and turnover, as well as deprotonation of 4NPA-CoA and 3S-C_8CoA αC−H. From experiments such as those depicted in Figures 5 and 6, the pK_a of the His376 imidazole is estimated as ≈9.3 (Table 3); i.e., the pK shift it experiences is even larger than that of Glu376. On the other hand, the αC−H pK_a of 3S-C_8CoA bound to this mutant is lowered to ≈7.6, i.e., by a substantially smaller amount compared to MCADH.

The microscopic pK_a of Glu376-COOH appears thus to be increased from ≈4.3 (free) by 2 units to ≈6.3 at the active center of uncomplexed MCADH (Table 3). On the basis of similar arguments and from the plots of Figure 5, the pK ≈7.3 (Figure 6) is assigned to Glu99-COOH in uncomplexed MCADH and that pK ≈8 to Glu99-COOH in ligand-associated MCADH (see also Scheme 3). The equilibria of Scheme 2 (excluding the part in brackets) are therefore linked:

$$K_{E-H}K_L = K_{L'}K_{E\sim L-H} \qquad (3)$$

That this relationship is valid can be verified by substitution with the experimentally derived values for the three ligands listed in Table 1.

For the αC−H deprotonation of 4NPA-CoA in aqueous medium, and on the basis of the pK_a of the acetonyl model,

Table 3: pK Values of αC−H and Enzyme Functional Groups and Shifts Induced upon Complex Formation

functional group	pK (free species)	pK at active center	ΔpK_a free/act. center (energ equiv, kJ mol^{-1})	pK (in presence of complexed ligand L)	ΔpK_a free/complex (energ equiv, kJ mol^{-1})
Glu-376-COOH	4.3	≈6.3	2 (12)	≈6 (4NPA-CoA)	2 (12)
				>6 (3S-C_8CoA)	>2 (>12)
				≥8 (substrate)[a]	≥4 (≥24)
His-376-imidazole[b]	6.0	9.3	3.3 (20)		
Glu-99-COOH	4.3	7.3	3 (18)	≈8 (4NPA-CoA)	≈4 (24)
3S-C_8CoA, ligand αC−H	≈16	5.1−5.2	≥11 (≥65)		
3′-dephospho-3S-C_8CoA, ligand αC−H	≈16	6.1	≥10 (≥60)		
4NPA-CoA, ligand αC−H	≥13.6	5.1	≥8.5 (≥50)		
C_8CoA, substrate αC−H	≈21	8−12[a]	9−13 (53−70)		

[a] Estimated value. [b] Values from Kieweg and Ghisla, unpublished results.

Scheme 3: Steps Involved in the Reaction of Ligand 4NPA-CoA (L−H) with MCADH[a]

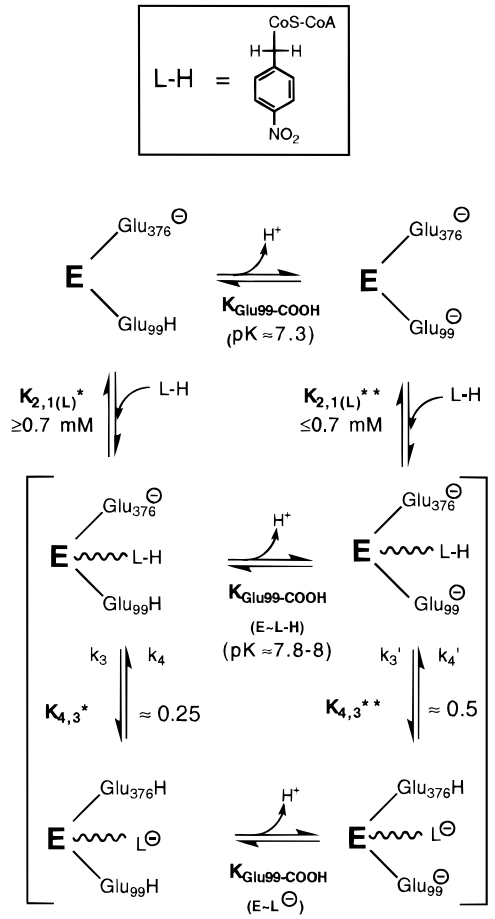

[a] For L−H, see structure inset. Steps $K_{2,1(L)}$* and $K_{2,1(L)}$** represent binding of L−H to enzyme in which Glu376-COO$^-$ is present and Glu99-COOH is either neutral (*, left branch) or ionized (**, right branch). Steps $K_{4,3}$* and $K_{4,3}$** are the ratios of the microscopic pK_as of Glu376-COOH and of bound L−H. For the values of single equilibrium constants see Tables 2 and 3, and see text for details.

a pK_a ≥ 13.6 can be assumed. The 3-thia sulfur of 3S-C_8-CoA lowers the pK_a of the adjacent α-proton by approximately 5 pK units compared to *n*-octanoyl-CoA (*16*), for which a pK_a ≈21 has been estimated (*8*, *9*). Hence, a pK_a ≈16 for the αC−H of free 3S-C_8CoA appears to be an educated guess. This leads to the estimation of the pK shifts for the αC−H dissociation of these ligands experienced upon binding to the active site of MCADH. These shifts are listed in Table 3 along with their energetic equivalents.

Comparison of Static and Rapid Reaction Data. The equilibrium described by K_L' in Scheme 2 consists of a binding step for L−H, described by the ligand binding equilibrium $K_{2,1(L-H)}'$, and the transfer of H$^+$ between the two partners (see Scheme 2, segment inside brackets). The steps in brackets are the reactions measured in the rapid reaction studies (Figures 7 and 8). The second of these steps, in turn, consists of the two microscopic ionizations:

$$\text{E-Glu376-COO}^- + \text{H}^+ \leftrightarrow \text{E-Glu376-COOH} \quad (1/K_{\text{E-Glu376-COOH}}) \qquad (4a)$$

$$\text{E}\sim\text{L}-\text{H} \leftrightarrow \text{E}\sim\text{L}^- + \text{H}^+ \quad (K_{\text{E}\sim\text{L}-\text{H}}) \qquad (4b)$$

which, combined, yield the transfer of H$^+$ from L−H to Glu376-COO$^-$:

$$\text{E-Glu376-COO}^- + \text{E}\sim\text{L}-\text{H} \leftrightarrow \text{E-Glu376-COOH} + \text{E}\sim\text{L}^- \quad (K_{3,4} = K_{\text{E}\sim\text{L}-\text{H}}/K_{\text{E-Glu376-COOH}}) \qquad (4c)$$

where the equilibrium constant of eq 4c is equivalent to the ratio of the corresponding microscopic dissociation constants. The latter, however, is equivalent to $1/K_{3,4} = K_{4,3}$ (see eq 2) and K_L' is thus described by

$$K_L' = K_{2,1(L)'}K_{4,3} = K_{2,1(L)'}K_{\text{E-Glu376-COOH}}/K_{\text{E}\sim\text{L}-\text{H}} \qquad (4d)$$

For 4NPA-CoA and Glu99Gly-MCADH and at pH 7.6, $K_{2,1(L)'}$ ≈50 μM and $K_{\text{E}\sim\text{L}-\text{H}}/K_{\text{Glu376}}$ ≈5; from this one obtains a calculated K_L' of 10 μM, which compares with the value of ≈25 μM obtained from static titrations (Table 1). This is a satisfactory coincidence in view of the difficulties inherent to the rapid reaction studies. With simpler words the microscopic p$K_{\text{E-Glu376-COOH}}$ in the complex with 4NPA-CoA is ≈6, i.e., ≈0.8 unit higher than p$K_{\text{E}\sim\text{L}-\text{H}}$ = 5.2, and more precisely:

$$K_{\text{E-Glu376-COOH}} = 0.17K_{\text{E}\sim\text{L}-\text{H}} \approx 1 \times 10^{-6}$$

This value is essentially the same as the pK_a estimated for Glu376-COOH in *uncomplexed* MCADH and it means that binding of this analogue does not markedly affect the latter pK_a.

The results obtained with 3S-C_8CoA can be interpreted in similar terms. However, in this case rapid reaction analysis is difficult due to the very fast rates, and there is no indication of k_4 having a finite value. In this case, the difference between the microscopic pKs (p$K_{\text{E-Glu376-COOH}}$ and p$K_{\text{E}\sim\text{L}-\text{H}}$) is thus larger and probably >1 pK unit, implying a pK > 6 for Glu376-COOH in the 3S-C_8CoA complex.

The case of the interaction of 4NPA-CoA with MCADH is somewhat more complicated due to the presence of the "additional" ionization of Glu99-COOH at the active center. The data are discussed referring to Scheme 3, in which the equilibria below pH 7, i.e., those involving the ionizations of Glu376-COOH and L−H (cf. Scheme 2, left-hand side), are omitted for clarity. Binding of ligand (L−H) occurs to enzyme in which Glu99-COOH is either neutral (left branch) or ionized (right) with the two species being linked by the corresponding dissociation (p$K_{\text{Glu99-COOH}}$ ≈7.3). The accuracy in the determination of the dissociation constants $K_{2,1(L-H)}$* and $K_{2,1(L-H)}$** from the rapid reaction kinetic data is not sufficient to detect a pH-dependent effect (cf. Figure 9A). The encounter complexes (center of Scheme 3) are linked by the pK of Glu99-COOH (≈8 from the static data of Figure 5B); they then react further by deprotonation of L−H via k_3 (at low pH) and k_3' (at high pH). The pH dependence of k_3 (Figure 9) is substantial (≈4-fold, Table 2) and reflects a pK ≈7.8, which is also observed with [α-$^2H_2$]-4NPA-CoA and is thus in good agreement with the statically determined one of ≈8. The rapid reaction studies depicted exemplarily in Figure 8 yield finite values for both k_3 and k_4, and according to the criteria discussed above for eq 4 the ratio $k_4/k_3 = K_{4,3}$ corresponds to the ratio of the ionizations $K_{\text{E-Glu376-COOH}}/K_{\text{E}\sim\text{L}-\text{H}}$. In other words the two

microscopic K_as differ by a pH-dependent factor of 2−4. This pH-dependent equilibrium is represented by the segment in brackets in Scheme 3. The ionization of Glu-99-COOH thus appears to increase the microscopic p*K* of 4NPA-CoA due to the repulsion of negative charges, and specifically, the major effect is a decrease in the rate of k_3. Thus, for neutral Glu-99-COOH $K_{4,3}$* ≈0.25 and this is very similar to that found with the Glu99Gly mutant (≈0.17). There is a fair correspondence between the kinetically estimated ratio $K_{4,3}$ and the ratio of ϵ_{CT1} and ϵ_{CT2}, the values estimated from static experiments of Figure 5A for the species at pH > and < 7.3, which should reflect the relative amount of anionic ligand in the complex (see also Figure 2, inset, absorption in the 500 nm area). A quantitative comparison, however, is not possible since the ionization state of Glu99-COOH also appears to affect to some extent the intrinsic ϵ_{CT} (Figure 2, inset, long-wavelength absorption).

The equilibria encompassed by the brackets of Scheme 3 should allow the estimation of the p*K* for the fourth ionization (bottom line), which should be that of Glu99-COOH in the complex with negatively charged ligand (as opposed to anionic Glu376COO^-). This p*K* should be increased by about 0.3 p*K* units from p*K* ≈7.8−8, that of Glu99-COOH in the presence of the charge on Glu376-COO^-. The experimentally observed effect of pH on k_4 is not significant (Figure 9B).

Interaction of 4NPA-CoA with Glu99-COOH. The behavior of the ligand 4NPA-CoA at the active center of MCADH can be rationalized on the basis of the active-site arrangement shown in Chart 1, which was modeled using the 3D coordinates reported by Kim et al. (*17*). The ligand occupies the same position as octanoyl-CoA, even though the fatty acid chain of the latter is flexible and the anionic form of 4NPA-CoA is planar and rigid. The -NO_2 group of 4NPA-CoA carries considerable negative charge density and lies within 2−3 Å of the carboxyl group of Glu-99 (Chart 1). Intriguingly, the pK_a attributed to the latter group does not show up with 3S-C_8CoA, at least not up to pH 9.5. The role of Glu99 is puzzling. While the group is too distant from the locus at which catalysis occurs to play a direct role, an interaction with Glu376 either directly or via water molecules could be envisaged. This could be analogous to the case of the double mutant Glu376Gly,Thr255Glu-MCADH, in which the catalytic Glu255 side chain is found in two different conformations, an "active" and a "resting" form (*45*). In the former the carboxylate is positioned close to the substrate αC−H, while in the latter it interacts with the carboxylate of Glu99 via hydrogen bonds (*45*). The failure of LCADH to show appreciable anion formation with these ligands as compared to MCADH is also puzzling, since, if taken at face value, it would indicate a less efficient substrate activation. This finding, on the other hand, corresponds to that of Hazekawa et al. (*21*), who have deduced from the IR frequencies of the thioester carbonyl a smaller extent of activation of acyl-CoAs bound to LCADH or IVDH as compared to MCADH or SCADH. That the different position of the catalytic Glu in the two groups of enzymes (*46*) affects the extent of activation of the thioester carbonyl is an attractive hypothesis.

The transition-state barrier for dehydrogenation of the physiological substrate *n*-octanoyl-CoA, based on an estimated k ≈1000 s^{-1} at 25 °C, is ≈56 kJ mol^{-1}. For free octanoyl-CoA, the microscopic αC−H pK_a value has been estimated as ≈20 (*8, 9*). The pK_a shift induced upon binding may thus be equivalent to or even greater than the ≈11 p*K* units observed with 3S-C_8CoA since for the latter a similar rate of αC−H deprotonation (k > 600 s^{-1})—which should reflect the extent of activation—was found (*19*). Similar arguments can be made for the substrate analogue *trans*-3-octenoyl-CoA studied by Thorpe and collaborators (*15*), for which a pK_a of ≈19 was estimated (*16*).

Chart 1: Mode of Binding of 4NPA-CoA to the Active Site of MCADH and Interaction with Glu99-COOH[a]

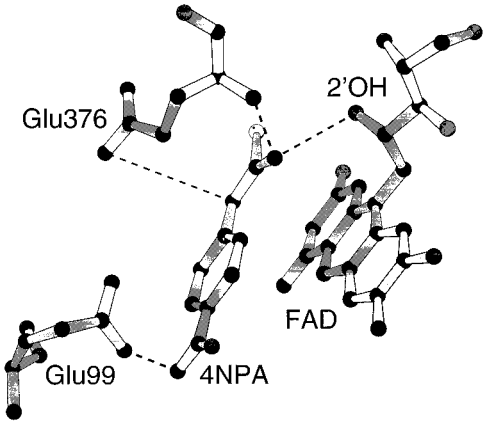

[a] The structure of anionic (4-nitrophenyl)acetate *S*-methyl ester was obtained using the geometry optimized routines MOPAC from the CAChe program (Textronix). The (4-nitrophenyl)acetyl molecule fragment was then linked to the CoA moiety at the active center of MCADH, the coordinates of which (complexed with product) are from Kim et al. (*17*). The aromatic moiety of 4NPA-CoA was arranged visually to optimize the interactions with amino acid side chains in the substrate binding pocket. The glutamic acid at position 99, which rotates almost 90° out of the active-site center upon binding of substrate/product, has been returned to the position occupied in uncomplexed enzyme to provide an interaction with the NO_2 group. The (not optimized) distance between the oxygen atoms of Glu-99-COOH and those of the *p*-NO_2 group is ≈2 Å. This suggests that upon binding some motion of the group(s) will occur in order to minimize this interaction. Note the short H-bond distances between the thioester carbonyl and the FAD-2′-OH (2.8 Å) and the Glu376N−H (3.0 Å) groups. The further type of interaction shown is that between Glu376-COOH and the analogue α-position. The 4NPA moiety is positioned in parallel to the isoalloxazine ring of the oxidized flavin system, the arrangement expected to give the CT interaction of the anion with the flavin. The diagram was obtained using the "O for Morons" program.

General Conclusions. The present data establish that the pK_a values of the αC−H of the acyl-CoA ligands 4NPA-CoA and 3S-C_8CoA are lowered by 8−12 p*K* units upon binding at the active center of MCADH (Table 3). The pK_a of the H^+-abstracting base, Glu376-COOH, is increased by ≈2 p*K* units at the active center and even further in the presence of ligand. The latter increase is estimated as >1 p*K* unit for 3S-C_8CoA and is most likely larger (≥2 p*K* units) for good substrates such as C_8CoA, while it cannot be quantified with 4NPA-CoA (Table 3). It thus appears that the effect is dependent on the nature of the ligand; indeed it might be "maximized at optimal chain length" as suggested by Trievel et al. (*9*) and by the pH dependence of activity on the substrate chain length (*47*). With good substrates such as C_8CoA and in the Michaelis complex the microscopic pK_as of substrate αC−H and E376-COOH thus appear to have similar values, and this is precisely what is required for efficient catalysis (*48*).

Substrate αC−H activation results from two short H-bonds interacting with the thioester carbonyl: one stems from the FAD ribityl-2′-OH and the second is from Glu376N−H (*17*). With 2′-deoxy-FAD-MCADH the rate of enzyme reduction is lowered ≈10^7-fold compared to normal, pig kidney MCADH (*18*, *19*). This would correspond energetically to ≈41 kJ mol^{-1}; thus the effect due to the ribityl-2′OH function would translate in a difference for the substrate αC−H microscopic p*K* of ≈7. It is thus most probable that these two H-bonds are crucial in originating the effect, the 2′-OH one being quantitatively more important. In view of this it is reasonable to assume that the apparent p*K* ≈8.2 (*48*, *49*) observed in the turnover of MCADH reflects (also) the ionization of Glu376-COOH in the Michaelis complex. This would mean that the two microscopic p*K*s in question are shifted from the values of the free species, i.e., ≈4 and ≈21, to within 2 units! The mechanism underlying the observed p*K* shifts is likely to involve the type of "low-barrier hydrogen bond" recently discussed by Gerlt and Gassman (*50*) and Cleland and Kreevoy (*51*).

ACKNOWLEDGMENT

We thank the reviewers for very helpful comments and Ms. M. Sappelt for skillfull technical assistance.

REFERENCES

1. Crane, F. L., Mii, S., Hauge, J. G., Green, D. E., and Beinert, H. (1956) *J. Biol. Chem. 218*, 701−716.
2. Beinert, H. (1963) in *The Enzymes, 2nd Ed.* (Boyer, P. D., Lardy, H., and Myrbäck, K., Eds.) Vol. 7, pp 447−476, Academic Press, New York.
3. Biellmann, J. F., & Hirth, C. G. (1970) *FEBS Lett. 9*, 55−56.
4. Biellmann, J. F., & Hirth, C. G. (1970) *FEBS Lett. 9*, 335−336.
5. Ghisla, S., Thorpe, C., & Massey, V. (1984) *Biochemistry 23*, 3154−3161.
6. Pohl, B., Raichle, T., and Ghisla, S. (1986) *Eur. J. Biochem. 160*, 109−115.
7. Kumar, N. R., and Srivastava, D. K. (1994) *Biochemistry 33*, 8833−8841.
8. Amyes, T. L., and Richard, J. P. (1992) *J. Am. Chem. Soc. 114*, 10297−10302.
9. Trievel, R. C., Wang, R., Anderson, V. E., and Thorpe, C. (1995) *Biochemistry 34*, 8597−8605.
10. Gerlt, J. A., Kozarich, J. W., Kenyon, G. L., and Gassman, P. G. (1991) *J. Am. Chem. Soc. 113*, 9667−9669.
11. Cornforth, J. W. (1959) *J. Lipid Res. 1*, 1−28.
12. Engel, P., and Massey, V. (1971) *Biochem. J. 125*, 889−902.
13. Ikeda, Y., Okamura-Ikeda, K., & Ikeda, K. (1985) *Biochemistry 24*, 7192−7199.
14. Fendrich, G., and Abeles, R. H. (1982) *Biochemistry 21*, 6685−6695.
15. Powell, P. J., Lau, S. M., Killian, D., and Thorpe, C. (1987) *Biochemistry 26*, 3704−3710.
16. Lau, S.-M., Brantley, R. K., and Thorpe, C. (1988) *Biochemistry 27*, 5089−5095.
17. Kim, J. J. P., Wang, M., and Paschke, R. (1993) *Proc. Natl. Acad. Sci. U.S.A. 90*, 7523−7527.
18. Ghisla, S., Engst, S., Moll, M., Bross, P., Strauss, A. W., and Kim, J.-J. P. (1992) in *New Developments in Fatty Acid Oxidation* (Coates, P. M., and Tanaka, K., Eds.) pp 127−142, Wiley-Liss, Inc., New York.
19. Engst, S. (1993) Ph.D. Thesis, University of Konstanz, Konstanz, Germany.
20. Nishina, Y., Sato, K., Hazekawa, I., and Shiga, K. (1995) *J. Biochem. (Tokyo) 117*, 800−808.
21. Hazekawa, I., Nishina, Y., Sato, K., Shichiri, M., and Shiga, K. (1995) *J. Biochem. (Tokyo) 118*, 900−910.
22. Thorpe, C., and Kim, J. J. (1995) *FASEB J. 9*, 718−725.
23. Engst, S., and Ghisla, S. (1991) in *Flavins and Flavoproteins 1990* (Curti, B., Ronchi, S., and Zanetti, G., Eds.) pp 311−314, Walter de Gruyter & Co., Berlin.
24. Sugai, S., Ikawa, H., Okazaki, T., Akabashi, S., & Ikegami, S. (1982) *Chem. Lett.*, 597−600.
25. Bellhof, D., and Mutter, M. (1984) *Polym. Bull. 11*, 49−54.
26. Jaeger, R., and Robinson, R. (1941) *J. Chem. Soc.*, 744−747.
27. Al-Arif, A., and Blecher, M. (1969) *J. Lipid Res. 10*, 344−345.
28. Goldmann, P., and Vagelos, P. R. (1961) *J. Biol. Chem. 236*, 2620−2623.
29. Ellman, G. L. (1959) *Arch. Biochem. Biophys. 82*, 70−77.
30. Kieweg, V., Kräutle, F.-G., Engst, S., Nandy, A., Vock, P., Abdel Ghani, A. G., Bross, P., Rasched, I., Strauss, A. W., and Ghisla, S. (1997) *Eur. J. Biochem. 246*, 548−556.
31. Eder, M., Kräutle, F. Y. D., Vock, P., Kieweg, V., Kim, J. J., Strauss, A. W., and Ghisla, S. (1996) *Eur. J. Biochem. 245*, 600−607.
32. Lehman, T. C., Hale, D. E., Bhala, A., & Thorpe, C. (1990) *Anal. Biochem. 186*, 280−284.
33. Schowen, B., and Schowen, R. L. (1982) *Methods Enzymol. 87*, 551−606.
34. Raichle, T. (1981) Ph.D. Thesis, University of Konstanz, Konstanz, Germany.
35. Fersht, A. (1985) in *Enzyme Structure and Mechanism*, pp 134−154, W. H. Freeman & Co., New York.
36. Strickland, S., Palmer, G., and Massey, V. (1975) *J. Biol. Chem. 250*, 4048−4052.
37. Chiang, Y., Kresge, A. J., & Tang, Y. S. (1984) *J. Am. Chem. Soc. 106*, 460−462.
38. Küchler, B., (1997) Ph.D. Thesis, University of Konstanz, Konstanz, Germany.
39. Auer, H. E., and Frerman, F. E. (1980) *J. Biol. Chem. 255*, 8157−8163.
40. Dixon, M., and Webb, E. C. (1979) *Enzymes*, pp 138−164, Longman Lt., Academic Press, New York.
41. Dixon, M. (1953) *Biochem. J. 55*, 161−170.
42. Chase, J. F. A., (1967) *Biochem. J. 104*, 503−509.
43. Johnson, B. D., Mancini, S. G., and Stankovich, M. T. (1995) *Biochemistry 34*, 7047−7055.
44. Ghisla, S., Engst, S., Vock, P., Kieweg, V., Bross, P., Nandy, A., Rasched, I. and Strauss, A. (1994) in *Flavins and Flavoproteins 1993: Proceedings of the Eleventh International Symposium, Nagoya* (Yagi, K., Ed.) pp 283−292, W. de Gruyter & Co., Berlin and New York.
45. Lee, H.-J., Wang, M., Paschke, R., Nandy, A., Ghisla, S., and Kim, J. J.-P. (1996) *Biochemistry 35*, 12412−12420.
46. Nandy, A., Küchler, B., and Ghisla, S. (1996) *Biochem. Soc. Trans. 24*, 105−110.
47. Ghisla, S., Braunwarth, A., and Vock, P. (1997) in *Flavins and Flavoproteins 1996* (Stevenson, K. J., Massey, V., and Williams, C. H., Jr., Eds.) pp 629−632, University of Calgary Press, Calgary, Alberta, Canada.
48. Gilbert, H. F. (1981) *Biochemistry 20*, 5643−5649.
49. Ghisla, S., Engst, S., Vock, P., Kieweg, V., Bross, P., Nandy, A., Rasched, I., and Strauss, A. W. (1994) in *Flavins and Flavoproteins: Proceedings of the Eleventh International Symposium* (Yagi, K., Ed.) pp 283−292, Walter de Gruyter & Co., Berlin.
50. Gerlt, J. A., and Gassman, P. G. (1993) *J. Am. Chem. Soc. 115*, 11552−11568.
51. Cleland, W. W., and Kreevoy, M. M. (1994) *Science 264*, 1887−1890.